

Direct high-precision mass spectrometry of superheavy elements with SHIPTRAP

O. Kaleja^{1,2,3,4,*} B. Andelić^{3,5,6} O. Bezrodnova,^{1,7,8} K. Blaum,¹ M. Block^{2,3,6} S. Chenmarev,^{2,7} P. Chhetri,^{3,9} C. Droese,^{3,4} Ch. E. Düllmann,^{2,3,6} M. Eibach,^{3,4} S. Eliseev,¹ J. Even,⁵ P. Filianin,¹ F. Giacoppo,^{3,6} S. Götz,^{2,3,6} Yu. Gusev,⁷ M. J. Gutiérrez¹⁰ F. P. Heßberger,^{3,6} N. Kalantar-Nayestanaki,⁵ J. J. W. van de Laar,^{2,3,6} M. Laatiaoui,^{2,3,6} S. Lohse,^{2,3,6} N. Martynova,^{7,8} E. Minaya Ramirez,¹¹ A. K. Mistry^{3,6} T. Murböck,³ Yu. Novikov,^{7,8} S. Raeder,^{3,6} D. Rodríguez¹⁰ F. Schneider,² L. Schweikhard,⁴ P. G. Thirolf,¹² and A. Yakushev^{3,6}

¹Max-Planck-Institut für Kernphysik, Saupfercheckweg 1, 69117 Heidelberg, Germany

²Department of Chemistry - TRIGA Site, Johannes Gutenberg University Mainz, Fritz-Strassmann-Weg 2, 55128 Mainz, Germany

³GSI Helmholtzzentrum für Schwerionenforschung, Planckstraße 1, 64291 Darmstadt, Germany

⁴Institut für Physik, Universität Greifswald, Felix-Hausdorff-Straße 6, 17489 Greifswald, Germany

⁵University of Groningen, Zernikelaan 25, 9747 AA Groningen, Netherlands

⁶Helmholtz-Institut Mainz, Staudingerweg 18, 55128 Mainz, Germany

⁷NRC Kurchatov Institute PNPI, Mkr. Orlova Roshcha 1, 188300 Gatchina, Russia

⁸Saint Petersburg State University, University Embankment 7/9, 199034 Saint Petersburg, Russia

⁹Technische Universität Darmstadt, Schloßgartenstraße 7, 64289 Darmstadt, Germany

¹⁰Departamento de Física Atómica, Molecular y Nuclear, Universidad de Granada, Avenida de la Fuente Nueva S/N, 18071 Granada, Spain

¹¹Université Paris-Saclay, CNRS/IN2P3, IJCLab, 91405 Orsay, France

¹²Ludwig-Maximilians-Universität München, Fakultät für Physik der LMU, Am Coulombwall 1, 85748 Garching, 80539 München, Germany



(Received 24 June 2022; accepted 28 September 2022; published 29 November 2022)

Direct mass measurements in the region of the heaviest elements were performed with the Penning-trap mass spectrometer SHIPTRAP at GSI Darmstadt. Utilizing the phase-imaging ion-cyclotron-resonance mass spectrometry technique, the atomic masses of ²⁵¹No ($Z = 102$), ²⁵⁴Lr ($Z = 103$), and ²⁵⁷Rf ($Z = 104$) available at rates down to one detected ion per day were determined directly for the first time. The ground-state masses of ²⁵⁴No and ^{255,256}Lr were improved by more than one order of magnitude. Relative statistical uncertainties as low as $\delta m/m \approx 10^{-9}$ were achieved. Mass resolving powers of 11 000 000 allowed resolving long-lived low-lying isomeric states from their respective ground states in ^{251,254}No and ^{254,255}Lr. This provided an unambiguous determination of the binding energies for odd- A and odd-odd nuclides previously determined only indirectly from decay spectroscopy.

DOI: [10.1103/PhysRevC.106.054325](https://doi.org/10.1103/PhysRevC.106.054325)

I. INTRODUCTION

The existence of superheavy elements (SHEs, proton number $Z \gtrsim 104$ –106) is understood as a consequence of quantum-mechanical nuclear shell effects that enhance their binding energy and half-lives. Different theoretical studies based on, e.g., relativistic mean-field calculations [1,2] or macroscopic-microscopic approaches [3–5] predict a so-called *island of stability*, an extended region of longer-lived

nuclei, around $Z = 114$, 120, or 126 and at $N = 172$ or 184 [6], depending on the model.

Atomic mass measurements provide nuclear binding energies and allow one to precisely determine parameters like two-nucleon separation energies, empirical shell gap parameters, and the nucleon pairing strength [7]. Such parameters reveal structural features and benchmark theoretical models that are used to extrapolate to properties of heavier and yet unknown nuclides. Reliable mass values of heavy nuclei are crucial for nuclear fission probabilities limiting the stellar nucleosynthesis in the r process [8–10]. Whether SHEs are produced in stellar environments remains a key question in nuclear physics [9,11–13]. In the laboratory, SHEs are produced in fusion-evaporation reactions. Limited available beam-target combinations prevent reaching more neutron-rich superheavy isotopes [14]. Thus, many superheavy nuclei, in particular those with $N = 184$, remain inaccessible for experiments and their atomic masses need to be either extrapolated based on

*Corresponding author: o.kaleja@gsi.de

Published by the American Physical Society under the terms of the [Creative Commons Attribution 4.0 International](https://creativecommons.org/licenses/by/4.0/) license. Further distribution of this work must maintain attribution to the author(s) and the published article's title, journal citation, and DOI. Open access publication funded by the Max Planck Society.

the regularity of the mass surface [15] or obtained from theoretical models [16].

Initially, the masses of nuclides with $Z > 100$ were obtained from measurements of their decay energies, requiring a direct link (*anchor point*) to the mass surface [17,18]. Many of these nuclides undergo α decay. For an α transition from the ground state of a mother nucleus ${}^A X$ to the ground state of its daughter nucleus ${}^{A-4} X'$ (mass number A and element symbols X and X') the Q value is determined by the measured energy of the emitted α particle taking into account the recoil energy of the daughter nucleus. Such ground-state-to-ground-state transitions are typically the strongest transitions for even-even nuclei. For odd-odd and odd- A nuclei, however, decays between states of similar configuration are preferred. Often, an excited state at an energy E^* is populated in the daughter nucleus, which deexcites into its ground state by γ emission or internal conversion. In some cases, the excited state might also decay by α emission. In these scenarios, the determination of the Q value from the measured emitted energies requires a comprehensive knowledge of the decay and level schemes of mother and (grand)daughter nuclei including energies of excited states. Excited states may be difficult to detect by means of decay spectroscopy if they are low-lying and long-lived, especially if they deexcite via highly converted transitions.

Direct high-precision mass spectrometry provides accurate masses from which Q values can be obtained accurately, independently of the decay mode and the knowledge of the nuclear level schemes. In the region of the SHEs such measurements suffer from low production rates, e.g., only few ions per month for ${}^{294}\text{Og}$ ($Z = 118$ and $N = 176$) [19], the heaviest known nuclide. Thus, experimental methods are required that feature highest overall efficiencies and highest detection sensitivities. High mass resolving powers and fast measurement times are required to identify low-lying isomeric states frequently occurring in this mass region [20].

Over a decade ago, pioneering experiments with SHIPTRAP demonstrated that Penning-trap mass spectrometry (PTMS) is feasible in very heavy nuclides [21–23]. Using the time-of-flight ion-cyclotron-resonance mass spectrometry (ToF-ICR MS) technique, ground-state masses of nobelium (No, $Z = 102$) and lawrencium (Lr, $Z = 103$) isotopes were measured with uncertainties down to $10 \text{ keV}/c^2$. The results pinned down the strength of the deformed neutron shell closure at $N = 152$ for $Z = 102$ [23] and provided reliable anchor points in this mass region. Recently, a multiple-reflection time-of-flight mass spectrometry (MR-ToF MS) experiment at RIKEN, Japan, also reached the heaviest elements, measuring the atomic masses of nuclides with $Z = 99$ – 102 [24] and $Z = 105$ with uncertainties between 46 and $266 \text{ keV}/c^2$, respectively [24,25]. In addition, ToF-ICR MS has been performed at TRIGATRAP on ${}^{241,243}\text{Am}$, ${}^{244}\text{Pu}$, and ${}^{249}\text{Cf}$ [26] with uncertainties on the order of $\approx 4 \text{ keV}/c^2$. However, despite all efforts, anchor points in the region of the heaviest elements remain sparse, as shown in Fig. 1.

II. EXPERIMENTAL SETUP

Here, we present the first application of the phase-imaging ion-cyclotron resonance mass spectrometry (PI-ICR MS)

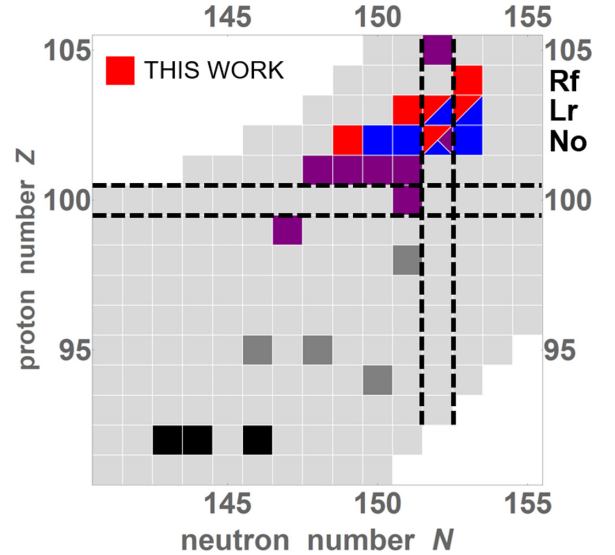


FIG. 1. Part of the nuclear chart, showing direct mass spectrometry carried out with the RIKEN MR-ToF MS (purple [24,25]), TRIGATRAP (dark gray), and SHIPTRAP [blue [21–23] and red (this work)]. Black and light gray squares represent stable nuclides and nuclides listed by the Atomic Mass Evaluation of 2020 (AME2020) [15], respectively. The black-dotted lines indicate deformed nuclear shell closures.

technique [38] in the SHE region with SHIPTRAP. The experimental setup has already been described in detail recently [39,40]. For the present studies, nobelium, lawrencium, and rutherfordium (Rf, $Z = 104$) isotopes were produced in fusion-evaporation reactions using ${}^{48}\text{Ca}$ and ${}^{50}\text{Ti}$ beams from the UNILAC accelerator [41]. Typical beam intensities on target were $\approx 8 \times 10^{12}$ and $\approx 4 \times 10^{12}$ particles per second, respectively. The projectiles irradiated $\approx 450 \mu\text{g}/\text{cm}^2$ (target material) thin layers of ${}^{209}\text{Bi}_2\text{O}_3$ and isotopically enriched (99.9%) ${}^{206,208}\text{PbS}$ evaporated onto thin C backings [42]. The primary-beam energy for each beam-target combination was chosen for maximum yield of the desired reaction product. Experimental key parameters are summarized in Table I. The cross section drops to 15 nb for ${}^{257}\text{Rf}$, corresponding to a

TABLE I. Half-lives $t_{1/2}$ [27], fusion-evaporation reactions, beam energies, and production cross sections σ of the nuclides included in the present study. The last column reports the excitation energy of known long-lived isomeric states, if present, directly disentangled from the corresponding ground state in this study. Beam energy is given in units of MeV/nucleon in front of the target.

Isotope	$t_{1/2}$ (s)	Reaction	Beam energy	σ (nb)	E_{exc} (keV)
${}^{251}\text{No}$	0.8	${}^{206}\text{Pb}({}^{48}\text{Ca}, 3n)$	4.80	30 [28]	≈ 106 [28]
${}^{254}\text{No}$	50	${}^{208}\text{Pb}({}^{48}\text{Ca}, 2n)$	4.56	2000 [29]	≈ 1295 [30]
${}^{254}\text{Lr}$	18.4	${}^{209}\text{Bi}({}^{48}\text{Ca}, 3n)$	4.81	25 [31]	≈ 108 [32]
${}^{255}\text{Lr}$	31.1	${}^{209}\text{Bi}({}^{48}\text{Ca}, 2n)$	4.56	250 [31]	≈ 37 [33]
${}^{256}\text{Lr}$	27	${}^{209}\text{Bi}({}^{48}\text{Ca}, 1n)$	4.50	60 [34]	
${}^{257}\text{Rf}$	4.4	${}^{208}\text{Pb}({}^{50}\text{Ti}, 1n)$	4.65	15 [35]	≈ 74 [36,37]

production rate of about one per minute in the focal plane of the velocity filter SHIP.

The fusion-evaporation reaction products were separated from the primary beam by the velocity filter SHIP [34] and penetrated through a ≈ 3.5 μm titanium entrance window foil into a cryogenic gas-stopping cell (CGC), operated at 45 K, in which they were stopped and thermalized in about 7 mbar helium gas [40,43]. The ions of interest were extracted predominantly as doubly charged ions and guided by electric fields into subsequent radiofrequency quadrupoles for cooling and bunching at typical helium buffer-gas pressures of 10^{-3} to 10^{-2} mbar. This section is also used to temporarily store ions of interest prior to their injection into a 7-T double Penning-trap system.

The first Penning trap employed a mass-selective buffer-gas cooling scheme [44]. In this work a modest mass resolving power of ≈ 2000 with cooling times of $t_{\text{prep}} \approx 200$ ms was sufficient. In the second Penning trap, the cyclotron frequency was obtained as the sum frequency $\nu_c = qB/(2\pi m) = \nu_- + \nu_+ = [\Delta\phi + 2\pi(n_- + n_+)]/(2\pi t_{\text{evo}})$ [45] of the magnetron (ν_-) and the modified cyclotron frequency (ν_+) in the Penning trap, measured by the phase difference $\Delta\phi \equiv (\phi_- - \phi_+)$ of both ion motions after the same phase-evolution time t_{evo} , where n_- and n_+ are integer numbers of full revolutions of the corresponding eigenmotion [38] which are determined by sufficiently low evolution times t_{evo} . The phase difference $\Delta\phi$ was determined by applying the excitation-pulse scheme as presented in Fig. 5 of [46] by axially ejecting the ions and transporting them to a position-sensitive microchannel-plate (MCP) detector.

Gaussian fits were applied to the x and y projections of the ion distribution from which the phase (angle) was calculated. The ion-optical transfer from the trap to the detector led to a projection with a 15-fold magnification. The typical width of the ion distributions (standard deviation) was ≈ 0.6 mm for radii of ≈ 10 mm on the MCP detector. The ions of interest had a well-defined time of flight to the detector with a full width at half maximum (FWHM) of about 1 μs . By applying gates for the time of flight of ± 1 μs and ± 2 mm (rectangular) for the radial position around the expected values, an appropriate background suppression to less than one background event per day at the expected detector position was achieved.

The overall efficiencies of ion detection (ratio between the ion rate behind SHIP and at the last MCP detector) ranged from 5% (for ^{254}No) to $<0.5\%$ (for ^{251}No and ^{257}Rf). The efficiency drop can be attributed to an increasing contamination level in the bunching section over the duration of the beam time, leading to increased ion-neutralization processes. This also restricted phase-evolution times to ≈ 40 ms for the measurement of ^{257}Rf . In addition, the entrance window's thickness increased over time due to the cryogenic operation (freezing of residual gas from the room-temperature vacuum of SHIP), which decreased the rate of ions entering the CGC [43].

Compared to the previously applied ToF-ICR MS method, the additional phase information of PI-ICR MS improves the mass resolving power and precision up to 40 times [46,47]. In addition, rather than detecting ions at different conversion frequencies to obtain a resonance around the expected cyclotron

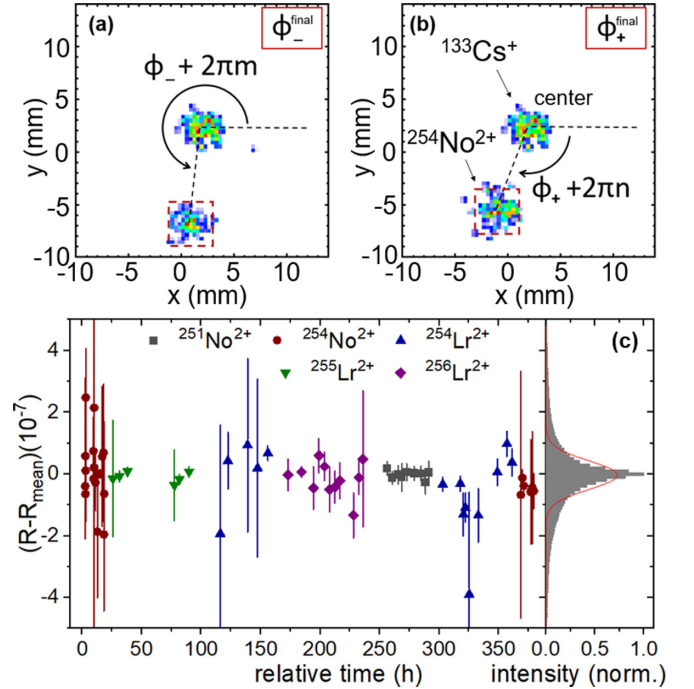


FIG. 2. Phase images of $^{254}\text{No}^{2+}$ ions after a phase-evolution time of ≈ 1188 ms (dashed red rectangles) for the magnetron motion (a) and the modified cyclotron motion (b). The images are superimposed with phase images of center measurements of $^{133}\text{Cs}^+$ ions. The individual frequency ratios for the nobelium and lawrencium isotopes of interest are symmetrically scattered around their mean value (c). The error bars correspond to the combined statistical and systematic uncertainty. For further details see text.

frequency ν_c , PI-ICR MS requires the detection of only single ions per radial phase to determine the cyclotron frequency, as the trap center can be determined using reference ions. Thus, the number of required ions for a mass measurement is 25 times smaller than with ToF-ICR MS [38].

III. ANALYSIS PROCEDURE

Figures 2(a) and 2(b) show a typical measurement for $^{254}\text{No}^{2+}$ at $t_{\text{evo}} \approx 1188$ ms. About 140 $^{254}\text{No}^{2+}$ ions were detected within 25 minutes yielding a relative uncertainty $\delta\nu_c/\nu_c = 3.5 \times 10^{-9}$ and a mass resolving power of $\approx 11\,000\,000$. The horizontal dashed lines define the zero degree angle, which can be chosen arbitrarily as only the relative phase difference of both radial phases in addition to the number of full magnetron and modified cyclotron revolutions is of relevance [38,46]. The overall measurement-cycle time is given by $t_{\text{cycle}} \approx t_{\text{prep}} + t_{\text{evo}}$. For short-lived nuclides below one second half-life, the phase-evolution time was reduced at the expense of mass resolving power and precision. Typical t_{cycle} varied from 0.3 to 1.5 s, whereas $t_{\text{evo}} \approx 500$ ms (in the case of $^{251}\text{No}^{2+}$), ≈ 40 to 1200 ms ($^{254}\text{No}^{2+}$), ≈ 30 to 600 ms ($^{254}\text{Lr}^{2+}$), ≈ 90 to 1500 ms ($^{255}\text{Lr}^{2+}$), and ≈ 70 to 1200 ms ($^{256}\text{Lr}^{2+}$). Figure 2(c) presents the difference between the obtained individual frequency ratios for the no-

TABLE II. Total number of detected ions, number of individual frequency measurements, uncertainty-weighted mean frequency ratios R_{mean} including systematic uncertainties, relative uncertainties, and mass excesses ME. ME_{lit} are the AME2020 values [15] and for ME_{new} the present results have been included in the atomic mass evaluation. All ME values are given in keV/c^2 .

Isotope	# ions	# meas	R_{mean}	Rel. unc.	$R_{\text{ToF-ICR}}$	Rel. unc.	ME	ME_{lit}	ME_{new}
^{251}No	39	9	0.944 614 687(9)	9.5×10^{-9}			82 851.3(23)	82 849(181)	82 851.1(21)
^{254}No	2448	24	0.955 908 554(6)	6.3×10^{-9}	0.955 908 520(60) [22]	6.3×10^{-8}	84 733.5(15)	84 723.3(97)	84 733.3(15)
					0.955 908 550(40) [23]	4.2×10^{-8}			
^{254}Lr	156	14	0.955 928 750(27)	2.8×10^{-8}			89 734.0(67)	89 645.9(913)	89 733.9(64)
^{255}Lr	278	6	0.959 691 642(7)	7.3×10^{-9}	0.959 691 740(60) [23]	6.3×10^{-8}	89 933.0(17)	89 947.3(177)	89 932.6(17)
^{256}Lr	124	11	0.963 461 017(23)	2.4×10^{-8}	0.963 461 0(3) [23]	3.1×10^{-7}	91 737.2(57)	91 746.6(829)	91 737.2(57)
^{257}Rf	5	2	0.967 240 149(670)	6.9×10^{-7}		-	95 960(170)	95 866.4(108)	95 866.4(108)

berium and lawrencium isotopes of interest and their resulting mean value.

To accurately determine the magnetic field, the cyclotron frequency of $^{133}\text{Cs}^+$ (reference ion) with well-known atomic mass [15] was measured. Thus, the cyclotron frequency ratio $R(^AX) = \nu_c(^{133}\text{Cs}^+)/\nu_c(^AX^{2+})$ between $^{133}\text{Cs}^+$ and the doubly-charged ions of interest $^AX^{2+}$ (with mass number A and element symbol X) are the primary experimental results. The bore temperature of the superconducting magnet and the pressure inside the liquid helium vessel were actively stabilized to the levels of 40 mK and 1 mbar, respectively. To account for magnetic field fluctuations, the cyclotron frequency of $^{133}\text{Cs}^+$ was measured before and after every measurement of the ion of interest and linearly interpolated to the time at which the ion of interest was measured. For nonlinear magnetic field fluctuations, a systematic uncertainty of $1.3 \times 10^{-9}/h \times \Delta t$ was taken into the error budget, where Δt equals the time difference between two reference ion measurements. This uncertainty was evaluated as described in [48], taking into account all reference measurements. In addition, linear interpolation as well as the polynomial method [49–52] have been applied. The results of both agree with similar uncertainties.

In addition, for every frequency measurement two center measurements (with $^{133}\text{Cs}^+$) before and after the measurement were linearly interpolated to account for possible electric-field fluctuations. The standard deviation of all center measurements of 0.3 mm was taken as the uncertainty for the interpolated center positions, which increased the uncertainties of the frequency measurements by ≈ 4 mHz. For ion-of-interest measurements in which only one ion has been detected in either of the phases, the standard deviation of typical spot sizes of 0.6 mm was taken as the uncertainty for the position. Due to low ion rates, ion-ion interactions are negligible in all cases, including $^{133}\text{Cs}^+$. Reference measurements typically took 5 min. Measurements of the ion of interest took between 5 min and 12 h depending on the ion detection rate.

The final result is an uncertainty-weighted mean of the individual frequency ratios that are subject to a mass-dependent systematic shift. This shift scales to first order linearly with the mass-to-charge difference between reference ion and ion of interest. A value of $3(6) \times 10^{-10}/(u/e)$ has been obtained for mass-to-charge ratio differences of up to 20 u/e by carrying out additional offline measurements using $^{116,118-120,124}\text{Sn}^+$ and $^{211}\text{Pb}^{2+}$ ions. As the maximum of the mass-to-charge

difference in the online measurements was 7.5 u/e , this systematic shift can be neglected in all cases. With the atomic mass of the reference ion $m(^{133}\text{Cs}^+)$ and the electron mass m_e [53], the atomic mass of the ion of interest is

$$m(^AX) = 2R(^AX) \times [m(^{133}\text{Cs}^+) - m_e] + 2m_e. \quad (1)$$

The electron binding energies on the order of few electronvolts are negligible with respect to the statistical precision. Our results are given as mass excesses $\text{ME}(^AX) = [m(^AX) - A \times u]c^2$ and summarized in Table II ($u = 931\,494.095(6)$ keV/c^2 [15] being the atomic mass unit). For $^{251,254}\text{No}$ and $^{254,255}\text{Lr}$ the long-lived isomeric states (cf. Table I) were separated from their respective ground states.

IV. EXPERIMENTAL RESULTS

^{251}No

After the discovery of ^{251}No in 1967 [54], the uncertainty of its Q_α value was successively reduced to 4 keV in the following decades by decay spectroscopy investigations [28]. However, the atomic mass uncertainty of ^{251}No was about two orders of magnitude higher [15], limited by the uncertainty of the atomic mass of ^{247}Fm . Our result of $\text{ME}(^{251}\text{No}) = 82\,851.3(23)$ keV/c^2 is consistent with the previously obtained atomic mass value of 82 849(181) keV/c^2 , reducing its uncertainty by about a factor of 82.

^{254}No

The measurement of ^{254}No is another example showing the accuracy improvement of PI-ICR MS compared to ToF-ICR MS and MR-ToF MS. The frequency ratio $R(^{254}\text{No}) = 0.955\,908\,554(6)$ with $\delta m/m \approx 6 \times 10^{-9}$ is in good agreement with the previous SHIPTRAP values of 0.955 908 520(60) [22] and 0.955 908 550(40) [23] using the same reference ion, reducing the uncertainty by a factor of 7. The corresponding mass excess is also in good agreement with results from decay-spectroscopy experiments [30,54–58], using the atomic mass from the latest atomic mass evaluation (AME) [15] of ^{250}Fm . In addition, the measurement time in this study was reduced to a fifth compared to the ToF-ICR MS campaign [21–23].

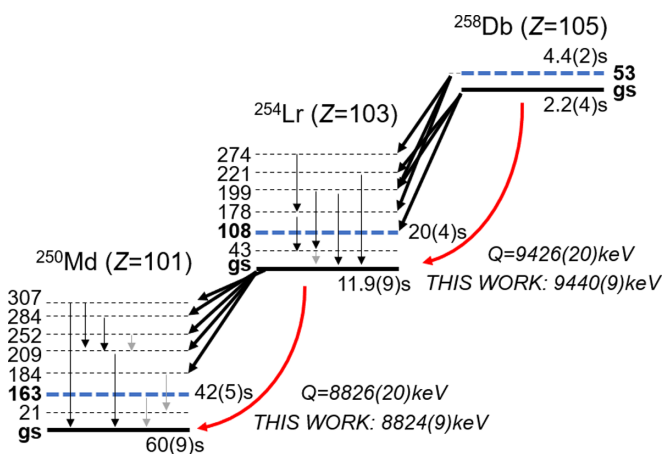


FIG. 3. Tentative decay and level schemes of the decay chain $^{258}\text{Db} - ^{254}\text{Lr} - ^{250}\text{Md}$ as proposed by [32] in which the literature Q values are compared with this work. The energies of excited states (dashed black lines) are given in keV and observed α and γ decays are represented as arrows. The thick blue dashed lines represent long-lived isomeric states and gray arrows indicate weak transitions. The half-lives for isomeric states are also given.

^{254}Lr

The atomic mass of ^{254}Lr has been measured directly for the first time, improving the precision by ≈ 50 with $M(^{254}\text{Lr}) = 89\,734.0(67)$ keV/ c^2 , and agrees well with literature [15]. Even though several decay-spectroscopy experiments have been performed over the past decades, the decay path of ^{254}Lr remained unclear, and only a tentative decay and level scheme has been presented recently [32]. As shown in Fig. 3, the odd-odd nuclei ^{258}Db , ^{254}Lr , and ^{250}Md are connected via α decays which nearly exclusively populate excited states in their daughters. Our atomic mass of ^{254}Lr , in combination with the atomic mass values of ^{250}Md and ^{258}Db from the AME2020 [15], agrees well with the tentative scheme presented in Fig. 3. Prior to our measurements, the atomic masses of these nuclei were extrapolated [15] with an uncertainty of 150 keV/ c^2 , which prevented distinguishing between different excited states.

^{255}Lr

The atomic mass of ^{255}Lr has been determined in previous SHIPTRAP experiments using ToF-ICR MS. Our frequency ratio with a relative uncertainty of 7.3×10^{-9} is ten times more precise and deviates from the previous result by 1.6σ .

This discrepancy can be explained by an admixture of the low-lying isomeric state at an excitation energy of about 37 keV (cf. Table I) in the ToF-ICR measurement. The ground state has a half-life of 31 s while the isomeric state has a half-life of 2.5 s [33]. The latter is comparable to typical measurement times in both the previously used ToF-ICR and the current PI-ICR measurements. In the previous ToF-ICR measurements, several resonances were taken using excitation times up to 4 s corresponding to mass resolving powers of about 10^6 [23], insufficient for separating the isomeric from the ground state. Assuming that the isomeric state is produced

in 1/3 of the cases, a contribution of less than 5% to the resonance of the ground state at an excitation time of 4 s was estimated. Therefore, a contribution of the isomeric state to the atomic mass of ^{255}Lr published in [23] was neglected. In this work, by applying PI-ICR at mass resolving powers of up to 1.1×10^7 , the isomeric state has been resolved, and it is shown that the production of the isomeric state has been underestimated in the previous ToF-ICR measurements. For similar production parameters, we find, based on our PI-ICR data, that at a measurement time of 4 s the isomeric state will contribute with an intensity of about 30% to a ToF-ICR resonance. This demonstrates that a sufficient mass resolving power is crucial to accurately determine atomic masses for nuclides with long-lived isomeric states.

^{256}Lr

In previous SHIPTRAP ToF-ICR MS measurements ^{256}Lr had been the most challenging nuclide due to the low detected ion rate below 0.5 ions/h [23]. A relative precision of 3.1×10^{-7} had been achieved, reducing the uncertainty of the ^{256}Lr atomic mass from 220 [59] to 80 keV/ c^2 [23]. Our present result with a relative uncertainty of 2.4×10^{-8} decreases this uncertainty by a factor of 13. Due to the implementation of the CGC, the detected ion rate for similar conditions was improved to ≈ 2 ions/h.

^{257}Rf

Five $^{257}\text{Rf}^{2+}$ events have been recorded at a rate of about one per day, allowing to determine the ground state mass of ^{257}Rf with an uncertainty of 170 keV/ c^2 . As its isomer at an excitation energy of ≈ 74 keV was not resolved and is known to be populated in the reaction by a large quantity of about 2/3 [36,37], it contributes to the atomic mass, which is reflected in the given uncertainty. Our result agrees with the mass published in AME2020 [15], extracted from the α decay of ^{257}Rf into ^{253}No .

The results from this work (cf. Table II) were incorporated into the AME2020 [15] to perform a new Atomic Mass Evaluation. The AME provides a comprehensive network of the mass surface. It is based on a least-square adjustment of all accepted experimental input data, e.g., from Q -value determinations, from decay spectroscopy, and mass values from direct mass spectrometry. Our results agree with the values listed in the AME. Including them improves the mass values of 15 additional nuclides indirectly. Five of them were previously based on the extrapolation of systematic trends (cf. Fig. 4). The heaviest affected isotope is ^{272}Rg with $Z = 111$, which is currently impossible to access in a direct mass measurement due to its milliseconds half-life and picobarn cross section [60].

The first direct mass measurements of the odd- A isotope ^{251}No and the odd-odd isotope ^{254}Lr serve as new anchor points in the region of the heaviest elements. This leads to improved mass values of the very short-lived isotopes ^{263}Hs and ^{266}Mt (both $\approx t_{1/2} = 0.8$ ms [61]), which have not been measured directly and will remain difficult to access by direct mass measurements due to their short lifetimes. Figure 4

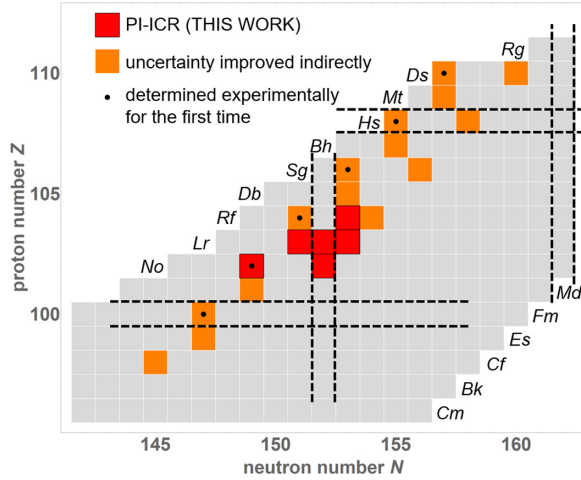


FIG. 4. AME evaluation including our new results. Gray squares indicate nuclides listed in the AME2020 [15]. Red squares represent the directly measured atomic masses of this work using PI-ICR. Orange squares represent nuclides for which the mass precision was improved indirectly by at least 10%. Black dots indicate nuclides for which the mass was determined experimentally for the first time. Dashed lines indicate nuclear shell closures. For further information see text.

presents an overview of the results of the AME evaluation for the heaviest elements.

The new mass values (cf. Fig. 4) enable an assessment of the evolution of the neutron shell gaps at $N = 152, 162$ [21,62] for different elements to determine the locality of these deformed shell closures. For this purpose, the two-neutron shell gap parameter $\delta_{2n}(Z, N) = S_{2n}(Z, N) - S_{2n}(Z, N + 2)$ [23], where $S_{2n}(Z, N)$ is the two-neutron separation energy, is evaluated for the shell closures $N = 152$ and $N = 162$ for $Z = 97-105$ and $Z = 106, 108, 110$, respectively (cf. Fig. 5). The size of the shell gap at $N = 152$ rises from about 1 MeV at $Z = 97$ to about 1.4 MeV at $Z = 101$ and drops slightly for $Z = 102$. The values for $Z = 103-105$ remain on a similar level, but their large uncertainties make it difficult to draw further conclusions on how far the shell gap extends. This shell closure is weak compared to spherical neutron shell closures, for example at $N = 126$ [15].

Albeit not directly measured, the updated mass values for linked nuclides confirm the existence of the neutron shell closure at $N = 162$ for nuclei as heavy as $Z = 110$. The two-neutron shell gap is of similar strength as for $N = 152$. Additional data for heavier nuclides are required to quantify the evolution of this shell gap with increasing proton number.

V. SUMMARY

For the first time, PI-ICR MS has been applied in the region of the heaviest nuclides. An unprecedented mass resolving power and high precision reduced the uncertainty compared to previous Penning-trap experiments by about one order of magnitude. This allowed the unambiguous determination of atomic ground-state masses with high accuracy excluding

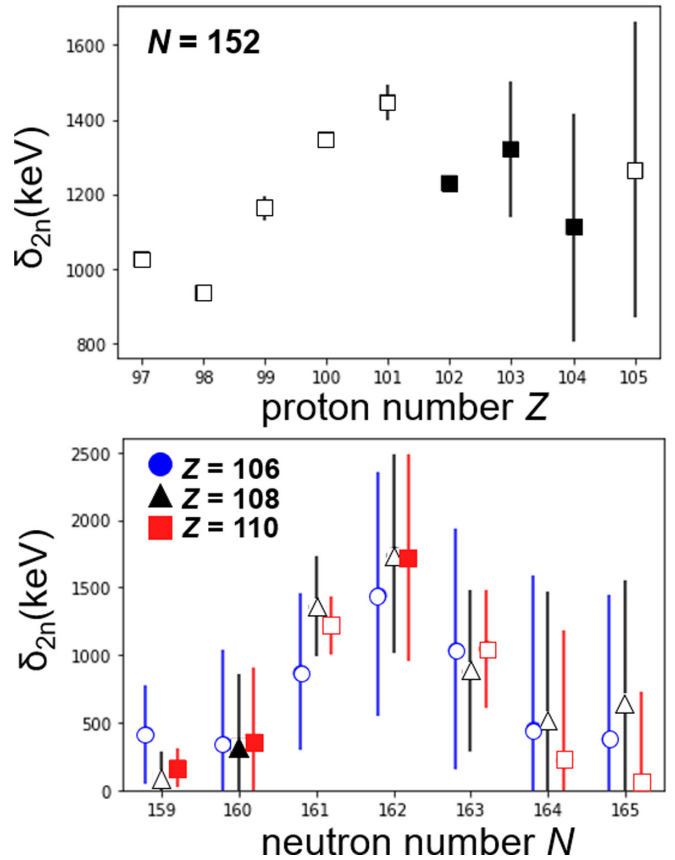


FIG. 5. Two-neutron shell gap parameter at $N = 152$ for $Z = 97-105$ (top figure) and two-neutron shell gap parameters for $Z = 106, 108, 110$ as a function of the neutron number (bottom figure) after the incorporation of our results into the AME. Data points are divided into filled (33% contribution from our work) and empty (no contribution). For further details see text.

contributions from long-lived low-lying isomeric states. The increased sensitivity allowed measuring the atomic mass of ^{257}Rf with only five ions in total at a detected ion rate of one ion per day. Four new anchor points, ^{251}No , $^{254,256}\text{Lr}$, and ^{257}Rf , were added to the atomic mass surface of this region. Based on these anchor points, 15 additional atomic masses were improved out of which 5 were determined experimentally for the first time. Our results confirm the shell gap strength at $N = 162$ to be comparable to that at $N = 152$.

ACKNOWLEDGMENTS

This article comprises results of the doctoral theses of O. Kaleja and B. Anđelić and is based on data obtained during online beam times in 2018 and offline measurements up to 2019 to study the systematic uncertainties. This experiment was carried out as part of FAIR-Phase-0 at the beam line Y7/SHIP at the GSI Helmholtzzentrum für Schwerionenforschung, Darmstadt, Germany. We thank the GSI ion source and accelerator staff for providing intense ion beams. In addition, we thank D. Racano, H.-G. Burkhard, and J. Maurer (GSI) for their supportive engineering work. We acknowledge financial support by the German BMBF (Grants

No. 05P15HGFNA, No. 05P19HGFNA, No. 05P21HGFN1, No. 05P15UMFNA, and No. 05P21UMFN1) and the Max-Planck Society. J.E. gratefully acknowledges financial support through NWO-natuurkunde Projectruimte grant (Project No. 680-91-103) and support from the Rosalind Franklin Fellowship program partly financed by the European Commission under Marie Skłodowska-Curie Action FP7 MSC COFUND scheme. M.L. acknowledges funding from the European

Research Council (ERC) under the European Union's Horizon 2020 research and innovation program (Grant Agreement No. 819957). D.R. and M.G. acknowledge support from the Spanish MICINN (Project No. FPA2015-67694-P and PID2019-104093GB-I00/AEI/10.01339/501100011033). We acknowledge M. Wang and W. Huang from the Institute of Modern Physics, Chinese Academy of Sciences in Lanzhou, China, for their atomic mass evaluation.

-
- [1] K. Rutz, M. Bender, T. Bürvenich, T. Schilling, P.-G. Reinhard, J. A. Maruhn, and W. Greiner, Superheavy nuclei in self-consistent nuclear calculations, *Phys. Rev. C* **56**, 238 (1997).
- [2] W. Zhang, J. Meng, S. Q. Zhang, L. S. Geng, and H. Toki, Magic numbers for superheavy nuclei in relativistic continuum Hartree-Bogoliubov theory, *Nucl. Phys. A* **753**, 106 (2005).
- [3] P. Moller, J. R. Nix, W. D. Myers, and W. J. Swiatecki, Nuclear ground-state masses and deformations, *At. Data Nucl. Data Tables* **59**, 185 (1995).
- [4] P. Möller, A. J. Sierk, T. Ichikawa, and H. Sagawa, Nuclear ground-state masses and deformations: FRDM(2012), *At. Data Nucl. Data Tables* **109-110**, 1 (2016).
- [5] I. Muntian, S. Hofmann, Z. Patyk, and A. Sobieczewski, Properties of heaviest nuclei, *Acta Phys. Pol. B* **34**, 2073 (2003).
- [6] A. Sobieczewski and K. Pomorski, Description of structure and properties of superheavy nuclei, *Prog. Part. Nucl. Phys.* **58**, 292 (2007).
- [7] G. Audi, The Evaluation of Atomic Masses, in *Atomic Physics at Accelerators: Mass Spectrometry* (Springer Netherlands, Dordrecht, 2001), pp. 7–34.
- [8] I. Petermann, K. Langanke, G. Martínez-Pinedo, I. V. Panov, P. G. Reinhard, and F. K. Thielemann, Have superheavy elements been produced in nature? *Eur. Phys. J. A* **48**, 122 (2012).
- [9] S. Goriely and G. Martínez Pinedo, The production of transuranium elements by the r -process nucleosynthesis, *Nucl. Phys. A* **944**, 158 (2015).
- [10] S. Goriely, The fundamental role of fission during r -process nucleosynthesis in neutron star mergers, *Eur. Phys. J. A* **51**, 1 (2015).
- [11] D. N. Schramm and W. A. Fowler, Synthesis of superheavy elements in the r -process, *Nature (London)* **231**, 103 (1971).
- [12] S. A. Giuliani, G. Martínez-Pinedo, and L. M. Robledo, Fission properties of superheavy nuclei for r -process calculations, *Phys. Rev. C* **97**, 034323 (2018).
- [13] S. A. Giuliani, G. Martínez-Pinedo, M.-R. Wu, and L. M. Robledo, Fission and the r -process nucleosynthesis of translead nuclei in neutron star mergers, *Phys. Rev. C* **102**, 045804 (2020).
- [14] V. I. Zagrebaev and W. Greiner, Production of heavy and superheavy neutron-rich nuclei in transfer reactions, *Phys. Rev. C* **83**, 044618 (2011).
- [15] M. Wang, W. J. Huang, F. G. Kondev, G. Audi, and S. Naimi, The AME 2020 atomic mass evaluation (II). Tables, graphs and references, *Chin. Phys. C* **45**, 030003 (2021).
- [16] K. Zhang, X. He, J. Meng, C. Pan, C. Shen, C. Wang, and S. Zhang, Predictive power for superheavy nuclear mass and possible stability beyond the neutron drip line in deformed relativistic Hartree-Bogoliubov theory in continuum, *Phys. Rev. C* **104**, L021301 (2021).
- [17] M. Asai, F. P. Heßberger, and A. Lopez-Martens, Nuclear structure of elements with $100 \leq Z \leq 109$ from alpha spectroscopy, *Nucl. Phys. A* **944**, 308 (2015).
- [18] Ch. Theisen, P. T. Greenlees, T.-L. Khoo, P. Chowdhury, and T. Ishii, In-beam spectroscopy of heavy elements, *Nucl. Phys. A* **944**, 333 (2015).
- [19] Yu. Ts. Oganessian, V. K. Utyonkov, Yu. V. Lobanov, F. Sh. Abdullin, A. N. Polyakov, R. N. Sagaidak, I. V. Shirokovsky, Yu. S. Tsyganov, A. A. Voinov, G. G. Gulbekian, S. L. Bogomolov, B. N. Gikal, A. N. Mezentsev, S. Iliev, V. G. Subbotin, A. M. Sukhov, K. Subotic, V. I. Zagrebaev, G. K. Vostokin, M. G. Itkis, K. J. Moody, J. B. Patin, D. A. Shaughnessy, M. A. Stoyer, N. J. Stoyer, P. A. Wilk, J. M. Kenneally, J. H. Landrum, J. F. Wild, and R. W. Lougheed, Synthesis of the isotopes of elements 118 and 116 in the ^{249}Cf and $^{245}\text{Cm} + ^{48}\text{Ca}$ fusion reactions, *Phys. Rev. C* **74**, 044602 (2006).
- [20] R.-D. Herzberg, P. T. Greenlees, P. A. Butler, G. D. Jones, M. Venhart, I. G. Darby, S. Eeckhaudt, K. Eskola, T. Grahn, C. Gray-Jones, F. P. Hessberger, P. Jones, R. Julin, S. Juutinen, S. Ketelhut, W. Korten, M. Leino, A.-P. Leppänen, S. Moon, M. Nyman, R. D. Page *et al.*, Nuclear isomers in superheavy elements as stepping stones towards the island of stability, *Nature (London)* **442**, 896 (2006).
- [21] M. Block, D. Ackermann, K. Blaum, C. Droese, M. Dworschak, S. Eliseev, T. Fleckenstein, E. Haettner, F. Herfurth, F. P. Heßberger, S. Hofmann, J. Ketelaer, J. Ketter, H.-J. Kluge, G. Marx, M. Mazzocco, Yu. N. Novikov, W. R. Plaß, A. Popeko, S. Rahaman *et al.* Direct mass measurements above uranium bridge the gap to the island of stability, *Nature (London)* **463**, 785 (2010).
- [22] M. Dworschak, M. Block, D. Ackermann, G. Audi, K. Blaum, C. Droese, S. Eliseev, T. Fleckenstein, E. Haettner, F. Herfurth, F. P. Heßberger, S. Hofmann, J. Ketelaer, J. Ketter, H.-J. Kluge, G. Marx, M. Mazzocco, Yu. N. Novikov, W. R. Plaß, A. Popeko, S. Rahaman, D. Rodríguez, C. Scheidenberger, L. Schweikhard, P. G. Thirof, G. K. Vorobyev, M. Wang, and C. Weber, Penning trap mass measurements on nobelium isotopes, *Phys. Rev. C* **81**, 064312 (2010).
- [23] E. M. Ramirez, D. Ackermann, K. Blaum, M. Block, C. Droese, Ch. E. Düllmann, M. Dworschak, M. Eibach, S. Eliseev, E. Haettner, F. Herfurth, F. P. Hessberger, S. Hofmann, J. Ketelaer, G. Marx, M. Mazzocco, D. Nesterenko, Y. N. Novikov, W. R. Plass, D. Rodriguez, C. Scheidenberger *et al.* Direct mapping of nuclear shell effects in the heaviest elements, *Science* **337**, 1207 (2012).

- [24] Y. Ito, P. Schury, M. Wada, F. Arai, H. Haba, Y. Hirayama, S. Ishizawa, D. Kaji, S. Kimura, H. Koura, M. MacCormick, H. Miyatake, J. Y. Moon, K. Morimoto, K. Morita, M. Mukai, I. Murray, T. Niwase, K. Okada, A. Ozawa, M. Rosenbusch *et al.*, First Direct Mass Measurements of Nuclides around $Z = 100$ with a Multireflection Time-of-Flight Mass Spectrograph, *Phys. Rev. Lett.* **120**, 152501 (2018).
- [25] P. Schury, T. Niwase, M. Wada, P. Brionnet, S. Chen, T. Hashimoto, H. Haba, Y. Hirayama, D. S. Hou, S. Imura, H. Ishiyama, S. Ishizawa, Y. Ito, D. Kaji, S. Kimura, H. Koura, J. J. Liu, H. Miyatake, J.-Y. Moon, K. Morimoto *et al.*, First high-precision direct determination of the atomic mass of a superheavy nuclide, *Phys. Rev. C* **104**, L021304 (2021).
- [26] M. Eibach, T. Beyer, K. Blaum, M. Block, Ch. E. Düllmann, K. Eberhardt, J. Grund, Sz. Nagy, H. Nitsche, W. Nörtershäuser, D. Renisch, K. P. Rykaczewski, F. Schneider, C. Smorra, J. Vieten, M. Wang, and K. Wendt, Direct high-precision mass measurements on $^{241,243}\text{Am}$, ^{244}Pu , and ^{249}Cf , *Phys. Rev. C* **89**, 064318 (2014).
- [27] Brookhaven National Laboratory National Nuclear Data Center, NuDat (Nuclear Structure and Decay Data), 2008.
- [28] F. P. Heßberger, S. Hofmann, D. Ackermann, S. Antalic, B. Kindler, I. Kojouharov, P. Kuusiniemi, M. Leino, B. Lommel, R. Mann, K. Nishio, A. G. Popeko, B. Sulignano, S. Saro, B. Streicher, M. Venhart, and A. V. Yeremin, Alpha-gamma decay studies of ^{255}Rf , ^{251}No and ^{247}Fm , *Eur. Phys. J. A* **30**, 561 (2006).
- [29] A. V. Belozеров, M. L. Chelnokov, V. I. Chepigin, T. P. Drobina, V. A. Gorshkov, A. P. Kabachenko, O. N. Malyshev, I. M. Merkin, Yu. Ts. Oganessian, A. G. Popeko, R. N. Sagaidak, A. I. Svirikhin, A. V. Yeremin, G. Berek, I. Brida, and Š. Šáro, Spontaneous-fission decay properties and production cross-sections for the neutron-deficient nobelium isotopes formed in the $^{44,48}\text{Ca} + ^{204,206,208}\text{Pb}$ reactions, *Eur. Phys. J. A* **16**, 447 (2003).
- [30] F. P. Heßberger, S. Antalic, B. Sulignano, D. Ackermann, S. Heinz, S. Hofmann, B. Kindler, J. Khuyagbaatar, I. Kojouharov, P. Kuusiniemi, M. Leino, B. Lommel, R. Mann, K. Nishio, A. G. Popeko, Š. Šáro, B. Streicher, J. Uusitalo, M. Venhart, and A. V. Yeremin, Decay studies of K isomers in ^{254}No , *Eur. Phys. J. A* **43**, 55 (2009).
- [31] F. P. Heßberger, GSI experiments on synthesis and nuclear structure investigations of the heaviest nuclei, *Eur. Phys. J. D* **45**, 33 (2007).
- [32] M. Vostinar, F. P. Heßberger, D. Ackermann, B. Andel, S. Antalic, M. Block, C. Droese, J. Even, S. Heinz, Z. Kalaninova, I. Kojouharov, M. Laatiaoui, A. K. Mistry, J. Piot, and H. Savajols, Alpha-gamma decay studies of ^{258}Db and its (grand)daughter nuclei ^{254}Lr and ^{250}Md , *Eur. Phys. J. A* **55**, 17 (2019).
- [33] A. Chatillon, Ch. Theisen, P. T. Greenlees, G. Auger, J. E. Bastin, E. Bouchez, B. Bouriquet, J. M. Casandjian, R. Cee, E. Clément, R. Dayras, G. de France, R. de Toureil, S. Eeckhaudt, A. Görgen, T. Grahn, S. Grévy, K. Hauschild, R. D. Herzberg, P. J. C. Ikin, G. D. Jones, P. Jones *et al.*, Spectroscopy and single-particle structure of the odd- Z heavy elements ^{255}Lr , ^{251}Md and ^{247}Es , *Eur. Phys. J. A* **30**, 397 (2006).
- [34] G. Münzenberg, W. Faust, S. Hofmann, P. Armbruster, K. Güttner, and H. Ewald, The velocity filter SHIP, a separator of unswelled heavy ion fusion products, *Nucl. Instrum. Methods* **161**, 65 (1979).
- [35] F. P. Heßberger, S. Hofmann, V. Ninov, P. Armbruster, H. Folger, G. Münzenberg, H. J. Schött, A. G. Popeko, A. V. Yeremin, A. N. Andreyev, and S. Saro, Spontaneous fission and alpha-decay properties of neutron deficient isotopes $^{257-253}\text{104}$ and $^{258}\text{106}$, *Z. Phys. A: Part. Fields* **359**, 415 (1997).
- [36] S. Jowzaee, S. Antalic, A. K. Mistry, D. Ackermann, B. Andel, M. Block, Z. Kalaninova, B. Kindler, I. Kojouharov, M. Laatiaoui, B. Lommel, J. Piot, and M. Vostinar, Alpha- and EC-decay measurements of ^{257}Rf , *Eur. Phys. J. A* **52**, 7 (2016).
- [37] K. Hauschild, A. Lopez-Martens, R. Chakma, O. Dorvaux, B. Gall, M. L. Chelnokov, V. I. Chepigin, A. V. Isaev, I. N. Izosimov, D. E. Katrasev, A. A. Kuznetsova, O. N. Malyshev, A. G. Popeko, Yu. A. Popov, E. A. Sokol, A. I. Svirikhin, A. V. Yeremin, D. Ackermann, J. Piot, P. Mosat, and B. Andel, Alpha-decay spectroscopy of ^{257}Rf , *Eur. Phys. J. A* **58**, 6 (2022).
- [38] S. Eliseev, K. Blaum, M. Block, C. Droese, M. Goncharov, E. Minaya Ramirez, D. A. Nesterenko, Yu. N. Novikov, and L. Schweikhard, Phase-Imaging Ion-Cyclotron-Resonance Measurements for Short-Lived Nuclides, *Phys. Rev. Lett.* **110**, 082501 (2013).
- [39] F. Giacoppo, K. Blaum, M. Block, P. Chhetri, Ch. E. Düllmann, C. Droese, S. Eliseev, P. Filianin, S. Götz, Y. Gusev, F. Herfurth, F. P. Hessberger, O. Kaleja, J. Khuyagbaatar, M. Laatiaoui, F. Lautenschläger, C. Lorenz, G. Marx, E. Minaya Ramirez, A. Mistry, Yu. N. Novikov, W. R. Plass, S. Raeder, D. Rodríguez *et al.* Recent upgrades of the SHIPTRAP setup: On the finish line towards direct mass spectroscopy of superheavy elements, *Acta Phys. Pol. B* **48**, 423 (2017).
- [40] O. Kaleja, B. Andjelić, K. Blaum, M. Block, P. Chhetri, C. Droese, Ch. E. Düllmann, M. Eibach, S. Eliseev, J. Even, S. Götz, F. Giacoppo, N. Kalantar-Nayestanaki, A. Mistry, T. Murböck, S. Raeder, and L. Schweikhard, The performance of the cryogenic buffer-gas stopping cell of SHIPTRAP, *Nucl. Instrum. Methods Phys. Res., Sect. B* **463**, 280 (2020).
- [41] W. Barth, W. Bayer, L. Dahl, L. Groening, S. Richter, and S. Yaramyshev, Upgrade program of the high current heavy ion UNILAC as an injector for FAIR, *Nucl. Instrum. Methods Phys. Res., Sect. A* **577**, 211 (2007).
- [42] B. Kindler, D. Ackermann, W. Hartmann, F. P. Heßberger, S. Hofmann, B. Lommel, R. Mann, and J. Steiner, Chemical compound targets for SHIP on heated carbon backings, *Nucl. Instrum. Methods Phys. Res., Sect. A* **561**, 107 (2006).
- [43] C. Droese, S. Eliseev, K. Blaum, M. Block, F. Herfurth, M. Laatiaoui, F. Lautenschläger, E. Minaya Ramirez, L. Schweikhard, V. V. Simon, and P. G. Thirolf, The cryogenic gas stopping cell of SHIPTRAP, *Nucl. Instrum. Methods Phys. Res., Sect. B* **338**, 126 (2014).
- [44] G. Savard, St. Becker, G. Bollen, H.-J. Kluge, R. B. Moore, Th. Otto, L. Schweikhard, H. Stolzenberg, and U. Wiess, A new cooling technique for heavy ions in a Penning trap, *Phys. Lett. A* **158**, 247 (1991).
- [45] L. S. Brown and G. Gabrielse, Geonium theory: Physics of a single electron or ion in a Penning trap, *Rev. Mod. Phys.* **58**, 233 (1986).
- [46] S. Eliseev, K. Blaum, M. Block, A. Dörr, C. Droese, T. Eronen, M. Goncharov, M. Höcker, J. Ketter, E. Minaya Ramirez, D. A. Nesterenko, Yu. N. Novikov, and L. Schweikhard, A phase-imaging technique for cyclotron-frequency measurements, *Appl. Phys. B* **114**, 107 (2014).
- [47] S. Eliseev, K. Blaum, M. Block, S. Chenmarev, H. Dorrer, Ch. E. Düllmann, C. Enss, P. E. Filianin, L. Gastaldo, M.

- Goncharov, U. Köster, F. Lautenschläger, Yu. N. Novikov, A. Rischka, R. X. Schüssler, L. Schweikhard, and A. Türlér, Direct Measurement of the Mass Difference of ^{163}Ho and ^{163}Dy Solves the Q -Value Puzzle for the Neutrino Mass Determination, *Phys. Rev. Lett.* **115**, 062501 (2015).
- [48] A. Kellerbauer, K. Blaum, G. Bollen, F. Herfurth, H.-J. Kluge, M. Kuckein, E. Sauvan, C. Scheidenberger, and L. Schweikhard, From direct to absolute mass measurements: A study of the accuracy of ISOLTRAP, *Eur. Phys. J. D* **22**, 53 (2003).
- [49] M. P. Bradley, J. V. Porto, S. Rainville, J. K. Thompson, and D. E. Pritchard, Penning Trap Measurements of the Masses of ^{133}C , $^{85,87}\text{Rb}$, and ^{23}Na with Uncertainties ≤ 0.2 ppb, *Phys. Rev. Lett.* **83**, 4510 (1999).
- [50] J. Karthein, D. Atanasov, K. Blaum, M. Breitenfeldt, V. Bondar, S. George, L. Hayen, D. Lunney, V. Manea, M. Mougeot, D. Neidherr, L. Schweikhard, N. Severijns, A. Welker, F. Wienholtz, R. N. Wolf, and K. Zuber, Q_{EC} -value determination for $^{21}\text{Na} \rightarrow ^{21}\text{Ne}$ and $^{23}\text{Mg} \rightarrow ^{23}\text{Na}$ mirror-nuclei decays using high-precision mass spectrometry with ISOLTRAP at the CERN ISOLDE facility, *Phys. Rev. C* **100**, 015502 (2019).
- [51] J. Karthein, D. Atanasov, K. Blaum, S. Eliseev, P. Filianin, D. Lunney, V. Manea, M. Mougeot, D. Neidherr, Y. Novikov, L. Schweikhard, A. Welker, F. Wienholtz, and K. Zuber, Direct decay-energy measurement as a route to the neutrino mass, *Hyperfine Interact.* **240**, 61 (2019).
- [52] A. Rischka, H. Cakir, M. Door, P. Filianin, Z. Harman, W. J. Huang, P. Indelicato, C. H. Keitel, C. M. König, K. Kromer, M. Müller, Y. N. Novikov, R. X. Schüssler, Ch. Schweiger, S. Eliseev, and K. Blaum, Mass-Difference Measurements on Heavy Nuclides with an eV/c^2 Accuracy in the PENTATRAP Spectrometer, *Phys. Rev. Lett.* **124**, 113001 (2020).
- [53] S. Sturm, F. Köhler, J. Zatorski, A. Wagner, Z. Harman, G. Werth, W. Quint, C. H. Keitel, and K. Blaum, High-precision measurement of the atomic mass of the electron, *Nature (London)* **506**, 467 (2014).
- [54] A. Ghiorso, T. Sikkeland, and M. J. Nurmi, Isotopes of Element 102 with Mass 251 to 258, *Phys. Rev. Lett.* **18**, 401 (1967).
- [55] V. L. Mikheev, V. I. Ilyushchenko, M. B. Miller, S. M. Polikanov, G. N. Flerov, and Yu. P. Kharitonov, Synthesis of isotopes of element 102 with mass numbers 254, 253, and 252, *Sov. At. Energy* **22**, 93 (1967).
- [56] F. P. Heßberger, G. Münzenberg, S. Hofmann, Y. K. Agarwal, K. Poppensieker, W. Reisdorf, K.-H. Schmidt, J. R. H. Schneider, W. F. W. Schneider, H. J. Schött, P. Armbruster, B. Thuma, C.-C. Sahm, and D. Vermeulen, The new isotopes $^{258}\text{105}$, $^{257}\text{105}$, ^{254}Lr and ^{253}Lr , *Z. Phys. A* **322**, 557 (1985).
- [57] C. M. Folden, S. L. Nelson, Ch. E. Düllmann, J. M. Schwantes, R. Sudowe, P. M. Zielinski, K. E. Gregorich, H. Nitsche, and D. C. Hoffman, Excitation function for the production of ^{262}Bh ($Z = 107$) in the odd- Z -projectile reaction $^{208}\text{Pb}(^{55}\text{Mn}, n)$, *Phys. Rev. C* **73**, 014611 (2006).
- [58] D. Kaji, K. Morimoto, Y. Wakabayashi, M. Takeyama, and M. Asai, First α - γ Spectroscopy Using Si-Ge Detector Array Installed at Focal Plane of GARIS, in *Proceedings of the Conference on Advances in Radioactive Isotope Science (ARIS2014)* [JPS Conf. Proc. **6**, 030106 (2015)].
- [59] G. Audi, O. Bersillon, J. Blachot, and A. H. Wapstra, The NUBASE evaluation of nuclear and decay properties, *Nucl. Phys. A* **729**, 3 (2003).
- [60] S. Hofmann, V. Ninov, F. P. Heßberger, P. Armbruster, H. Folger, G. Münzenberg, H. J. Schött, A. G. Popeko, A. V. Yeremin, A. N. Andreyev, S. Saro, R. Janik, and M. Leino, The new element 111, *Z. Phys. A* **350**, 281 (1995).
- [61] F. P. Hessberger, GSI experiments in the region of heaviest elements, *J. Phys. G: Nucl. Part. Phys.* **25**, 877 (1999).
- [62] Yu. A. Lazarev, Yu. V. Lobanov, Yu. Ts. Oganessian, V. K. Utyonkov, F. Sh. Abdullin, A. N. Polyakov, J. Rigol, I. V. Shirokovsky, Yu. S. Tsyganov, S. Iliev, V. G. Subbotin, A. M. Sukhov, G. V. Buklanov, B. N. Gikal, V. B. Kutner, A. N. Mezentsev, K. Subotic, J. F. Wild, R. W. Lougheed, and K. J. Moody, α decay of $^{110}\text{273}$: Shell closure at $N = 162$, *Phys. Rev. C* **54**, 620 (1996).